The phase diagram of the XXZ model for slab and layered geometries

1991 J. Phys.: Condens. Matter 3 9995

(http://iopscience.iop.org/0953-8984/3/50/006)

J. Phys.: Condens. Matter 3 (1991) 9995–10020. Printed in the UK

The phase diagram of the XXZ model for slab and layered geometries

Dirk Jan Bukman and J M J van Leeuwen

Instituut-Lorentz, Rijksuniversiteit te Leiden, PO Box 9506, 2300 RA Leiden, The Netherlands

Received 29th July 1991

Abstract. The phase diagram of the spin-$\frac{1}{2}$ XXZ model is examined for two different geometries, which can be changed from two- to three-dimensional. The first of these consists of an infinite stack of simple quadratic layers with a variable inter-layer coupling, where the ratio of the inter-layer and intra-layer couplings varies between zero and one. Second, we consider a slab geometry consisting of n such layers, with equal couplings in all directions. For both geometries we use the cluster variation method for two-spin clusters to construct the phase diagram of the model, and we examine the changes that take place as the system changes from two- to three-dimensional. For the slab geometry we also calculate the order parameter profile near T_c. It turns out that Dirichlet boundary conditions for the related superfluid wavefunction are most realistic.

1. Introduction

The behaviour of systems as a function of their spatial dimension is an important issue in statistical physics. Indeed, some properties, like critical exponents and the existence of a phase transition, depend almost exclusively on the spatial dimension and the symmetry of the model. Many of these quantities have been accurately calculated, e.g. with momentum-space renormalization techniques. In addition to these so-called universal properties, there are also quantities such as the critical temperature, that *do* depend on the details of the geometry and the Hamiltonian of the model. In some cases real-space renormalization has been successful in calculating these properties. Also, various series expansion methods have achieved a high accuracy in examining some specific models. For quantum spin models, however, real-space renormalization runs into considerable difficulties, while series expansions cannot give a global picture of the whole phase diagram of more complicated models. This is why practically the only general method used to deal with such models is the mean-field approximation. Since this method gives only a crude approximation of the phase diagram, more sophisticated approaches are needed. In this paper we use a more refined method to calculate phase diagrams and to study the influence of the spatial dimension on the details of these diagrams.

In order to study the influence of the dimension on the behaviour of a system, one may consider geometries that can be made to cross over between different dimensions. We will examine two quantum spin models that can be changed from two- to three-dimensional by varying a parameter of the model. In the first model we consider how a collection of uncoupled two-dimensional layers changes into a fully isotropic

0953-8984/91/509995+26$03.50

three-dimensional system as the inter-layer coupling is turned on. Second, we turn to a model consisting of a slab of n such layers, which becomes three-dimensional as its width approaches infinity. For both models, we will examine the changes in the phase diagram as these parameters are varied.

The specific spin model we will be studying is the spin-$\frac{1}{2}$ XXZ model. Its Hamiltonian is

$$\mathcal{H} = \sum_{\langle ij \rangle} -J_{ij}(\sigma_i^x \sigma_j^x + \sigma_i^y \sigma_j^y) - J_{z\,ij}\sigma_i^z \sigma_j^z - \sum_{i=1}^{N} h\sigma_i^z \,. \tag{1.1}$$

The sum $\sum_{\langle ij \rangle}$ is over nearest-neighbour spins only, and the σ_i^α are Pauli matrices. The spin coupling is anisotropic in spin space, i.e. $J_{ij} \neq J_{z\,ij}$, and by choosing J_{ij} and $J_{z\,ij}$ to be different for different pairs of spins i and j, it can also be made anisotropic in real space. In addition to the coupling there is a homogeneous magnetic field h in the z direction. We will consider bipartite lattices only, so an antiferromagnetic phase can always be accommodated without having to take frustration into account. For such a lattice we can assume that J_{ij} is positive, i.e. ferromagnetic, since the model is invariant under a change of sign of J_{ij} [1]. (We do not consider cases where different J_{ij} or $J_{z\,ij}$ have different signs.)

The Hamiltonian (1.1) is of interest for two reasons. First, it is interesting in itself, having two competing interactions, J and J_z, and both a continuous symmetry, for rotations of the spins around the z-axis, and a discrete up-down symmetry if $h = 0$. It also comprises various special cases like the Ising, Heisenberg, and XY models. Second, it is the Hamiltonian one obtains when writing a simple lattice gas model of a fluid consisting of interacting hard core bosons in the pseudo-spin formulation [1, 2]. As such, it has been used to examine both superfluidity [2–4] and superconductivity [5–8], the latter in the framework of theories that assume the existence of preformed, real-space pairs in high-T_c superconductors. Apart from the obvious interpretation of the spin model as a magnetic system in a layered or film geometry, one could then also make a connection with superconductors that consist of weakly coupled layers, or superfluid films of ^{4}He. This model is much too simplified, however, to give more than a qualitative picture of such systems.

The method we use to construct the phase diagram of the spin system is the cluster variation method using two-spin clusters. This method can be viewed as an extension of the mean-field approximation that also takes into account the correlations between neighbouring spins. It is the quantum version of Kikuchi's variational method for classical spins [9–11], and it is essentially a mean-field-like method; e.g. it reproduces the mean-field values of the critical exponents. For getting a global picture of the phase diagram it is a considerable improvement over the mean-field approximation, which is one of the few general methods applied to the Hamiltonian (1.1) so far. The cluster variation method has turned out to give quite good results for the phase diagrams of fully isotropic two- and three-dimensional quantum spin models [12, 13], despite some unphysical behaviour at low temperature.

In section 2 we will give a description of the cluster variation method, and then, in sections 3 and 4, apply it to the two geometries mentioned above. The results are discussed in section 5.

2. General theory

In this section we briefly outline the cluster variation method that is described in

more detail in [13]. The starting point of this method is the variational principle for the free energy $\mathcal{F}$ as a functional of the density matrix ρ of a system

$$\mathcal{F}[\rho] = \mathrm{Tr}(\rho\mathcal{H}) + k_B T \,\mathrm{Tr}(\rho \ln \rho)\,. \tag{2.1}$$

The density matrix must satisfy $\mathrm{Tr}\rho = 1$, and for the true density matrix ρ_0 that minimizes $\mathcal{F}$ one finds for the free energy

$$F = \min_{\rho} \mathcal{F}[\rho] = \mathcal{F}[\rho_0] = E - TS\,. \tag{2.2}$$

An approximation can be made by expanding $\mathcal{F}$ in cumulants, and only considering the reduced density matrices $\rho_C^{(n)}$ for a limited set of small clusters C. The reduced density matrix for a cluster C containing n spins is

$$\rho_C^{(n)} = \mathop{\mathrm{Tr}}_{\text{spins}\notin C} \rho \tag{2.3}$$

where all spins not in C are traced out. We will limit ourselves to clusters consisting of single spins and nearest-neighbour pairs.

For a Hamiltonian like (1.1) that only contains on-site terms $h_i^{(1)}$ and nearest-neighbour interactions $h_{ij}^{(2)}$, one can, in this approximation, express $\mathcal{F}$ in terms of $\rho_i^{(1)}$ and $\rho_{ij}^{(2)}$ as follows:

$$\mathcal{F} = \sum_{i=1}^{N} \mathrm{Tr}(\rho_i^{(1)} h_i^{(1)}) + \sum_{\langle ij\rangle} \mathrm{Tr}(\rho_{ij}^{(2)} h_{ij}^{(2)}) - T\left\{ \sum_{i=1}^{N} S_i^{(1)} + \sum_{\langle ij\rangle} \left(S_{ij}^{(2)} - S_i^{(1)} - S_j^{(1)} \right) \right\} \tag{2.4}$$

where the so-called cluster entropies $S_i^{(1)}$ and $S_{ij}^{(2)}$ are defined as

$$S_i^{(1)} \equiv -k_B \mathrm{Tr}(\rho_i^{(1)} \ln \rho_i^{(1)}) \tag{2.5}$$

$$S_{ij}^{(2)} \equiv -k_B \mathrm{Tr}(\rho_{ij}^{(2)} \ln \rho_{ij}^{(2)})\,. \tag{2.6}$$

These quantities are the most convenient from a calculational point of view, since they involve only a single reduced density matrix. All equivalent clusters have the same cluster entropy, and the number of non-equivalent clusters is determined by the geometry of the lattice and the phase that one wants to describe. In order to have the possibility to describe an antiferromagnetic phase we must at least distinguish between $S_{i\,a}^{(1)}$ and $S_{i\,b}^{(1)}$, where a and b are the two sublattices of the bipartite lattice. In a more complicated geometry there will be more types of one-spin clusters, and also several different types of nearest-neighbour pairs, each with its own cluster entropy $S_{ij}^{(2)}$. This will be the case when we consider the anisotropic and layered geometries in sections 3 and 4.

What remains to be done is to find a suitable parametrization for the reduced density matrices. In dealing with a spin-$\frac{1}{2}$ system one can always express these matrices in terms of Pauli spin matrices:

$$\rho_i^{(1)} = \tfrac{1}{2}\Big(1 + \sum_\alpha c_i^\alpha \sigma_i^\alpha\Big) \qquad (\alpha = x, y, z)$$
$$\rho_{ij}^{(2)} = \tfrac{1}{4}\Big(1 + \sum_\alpha (c_i^\alpha \sigma_i^\alpha + c_j^\alpha \sigma_j^\alpha) + \sum_{\alpha,\beta} c_{ij}^{\alpha\beta} \sigma_i^\alpha \sigma_j^\beta\Big) \qquad (\alpha, \beta = x, y, z)\,. \tag{2.7}$$

The functional $\mathcal{F}$ is now a function of the parameters c_i^α and $c_{ij}^{\alpha\beta}$. These parameters are just the averages of the spin operators, $c_i^\alpha = \mathrm{Tr}(\rho_i^{(1)}\sigma_i^\alpha) = \langle\sigma_i^\alpha\rangle$, and likewise $c_{ij}^{\alpha\beta} = \langle\sigma_i^\alpha\sigma_j^\beta\rangle$. From the symmetry of the Hamiltonian and of the phases under consideration one can deduce two properties of these parameters. First, not all of them are independent (e.g. one can take $c_i^x = c_i^y$ and $c_{ij}^{xx} = c_{ij}^{yy}$ etc. because of the rotation symmetry around the z-axis in spin space of (1.1)). Second, some of the parameters are characteristic of the ordered phases of the system, i.e. they are only non-zero when a symmetry in the Hamiltonian is spontaneously broken. The most important of these is the order parameter of the ordered phase. We will refer to these parameters characteristic of an ordered phase as 'order' parameters. The parameters can be classified accordingly:

(i) In the disordered, high temperature phase only c_{ij}^{xx} and c_{ij}^{zz} and, provided that $h \neq 0$, the magnetization $m_i \equiv \frac{1}{2}(c_{ia}^z + c_{ib}^z)$ are non-zero. There is no spontaneous breaking of any of the symmetries of the Hamiltonian.

(ii) For negative values of J_z the system can order antiferromagnetically in the z-direction. The order parameter of this antiferromagnetic Ising phase is the staggered magnetization $\bar{m}_i \equiv \frac{1}{2}(c_{ia}^z - c_{ib}^z)$.

(iii) If the x–y rotation symmetry is spontaneously broken, the system has a non-zero magnetization in the x–y plane. The order parameter for this x–y ordered phase is c_i^x, while the other 'order' parameters are c_{ij}^{xz}, c_{ij}^{zx}, and c_{ij}^{xy}.

(iv) In the case that $h = 0$ there is a phase where the spins order spontaneously in the z-direction. The order parameter for this ferromagnetically ordered Ising phase is m_i. In the following we will generally assume that $h \neq 0$, and occasionally make a remark concerning the case $h = 0$.

We can express the reduced density matrices in these parameters as follows (the bases $\{|+\rangle, |-\rangle\}$ and $\{|++\rangle, |+-\rangle, |-+\rangle, |--\rangle\}$ have been used):

$$\rho_i^{(1)} = \tfrac{1}{2}\begin{pmatrix} 1 + c_i^z & (1-i)c_i^x \\ (1+i)c_i^x & 1 - c_i^z \end{pmatrix}$$

$$\rho_{ij}^{(2)} = \tfrac{1}{4}\begin{pmatrix} 1 + c_i^z + c_j^z + c^{zz} & (1-i)(c_j^x + c^{zx}) & (1-i)(c_i^x + c^{xz}) & -2ic^{xy} \\ (1+i)(c_j^x + c^{zx}) & 1 + c_i^z - c_j^z - c^{zz} & 2c^{xx} & (1-i)(c_i^x - c^{xz}) \\ (1+i)(c_i^x + c^{xz}) & 2c^{xx} & 1 - c_i^z + c_j^z - c^{zz} & (1-i)(c_j^x - c^{zx}) \\ 2ic^{xy} & (1+i)(c_i^x - c^{xz}) & (1+i)(c_j^x - c^{zx}) & 1 - c_i^z - c_j^z + c^{zz} \end{pmatrix} \tag{2.8}$$

where we have, for clarity, omitted the label ij for the parameters $c_{ij}^{\alpha\beta}$ in the expression for $\rho_{ij}^{(2)}$. While it is easy to calculate the energy part in (2.4) with these expressions, for the entropy part we need to evaluate traces like

$$\mathrm{Tr}(\rho \ln \rho) = \sum_k \lambda_k \ln \lambda_k \tag{2.9}$$

where λ_k are the eigenvalues of the matrix ρ. It was shown in [13] that, if one is only interested in locating the phase boundaries, it suffices to calculate the eigenvalues perturbatively up to second-order in the x–y 'order' parameters c_i^x, c_{ij}^{xz}, and c_{ij}^{zx}. For a continuous transition one can then find the boundaries between the ordered phases and the disordered high temperature phase, since these parameters are small near the phase boundaries. The first order term λ_k^1 turns out to be zero, and one finds for the eigenvalues

$$\lambda_k = \lambda_k^0 + \lambda_k^2 + \mathrm{O}(c^{x4}) \tag{2.10}$$

and hence for the trace (2.9)

$$\mathrm{Tr}(\rho \ln \rho) = \sum_k \lambda_k \ln \lambda_k = \sum_k (\lambda_k^0 + \lambda_k^2) \ln \lambda_k^0 + \mathrm{O}(c^{x4}) . \tag{2.11}$$

The eigenvalues μ one finds in this way for $\rho_i^{(1)}$ are

$$\begin{aligned} \mu_{i1}^0 &= \tfrac{1}{2}(1 + c_i^z) \qquad & \mu_{i2}^0 &= \tfrac{1}{2}(1 - c_i^z) \\ \mu_{i1}^2 &= \frac{c_i^{x2}}{2c_i^z} \qquad & \mu_{i2}^2 &= -\frac{c_i^{x2}}{2c_i^z} . \end{aligned} \tag{2.12}$$

To zeroth order the eigenvalues λ_{ij} of $\rho_{ij}^{(2)}$ are (again dropping the label ij)

$$\begin{aligned} \lambda_1^0 &= \tfrac{1}{4}(1 + c_i^z + c_j^z + c^{zz}) \\ \lambda_2^0 &= \tfrac{1}{4}\{1 + [(c_i^z - c_j^z)^2 + 4c^{xx2}]^{1/2} - c^{zz}\} \\ \lambda_3^0 &= \tfrac{1}{4}\{1 - [(c_i^z - c_j^z)^2 + 4c^{xx2}]^{1/2} - c^{zz}\} \\ \lambda_4^0 &= \tfrac{1}{4}(1 - c_i^z - c_j^z + c^{zz}) . \end{aligned} \tag{2.13}$$

The second-order terms are

$$\lambda_k^2 = \frac{1}{8(1+\xi^2)} \left\{ \frac{P_{km}}{\lambda_k^0 - \lambda_m^0} + \frac{P_{kn}}{\lambda_k^0 - \lambda_n^0} \right\} \tag{2.14}$$

with $m = 2$, $n = 3$ for $k = 1$, 4 and $m = 1$, $n = 4$ for $k = 2$, 3, and where ξ is defined by

$$\xi \equiv \frac{c_i^z - c_j^z}{2c^{xx}} \left[\left(1 + \frac{4c^{xx2}}{(c_i^z - c_j^z)^2} \right)^{1/2} - 1 \right] . \tag{2.15}$$

The P_{km} are given by

$$\begin{aligned} P_{12} = P_{21} &= \left[c_j^x + c^{xx} + \xi(c_i^x + c^{xx})\right]^2 \\ P_{13} = P_{31} &= \left[c_i^x + c^{xx} - \xi(c_j^x + c^{xx})\right]^2 \\ P_{24} = P_{42} &= \left[c_i^x - c^{xx} + \xi(c_j^x - c^{xx})\right]^2 \\ P_{34} = P_{43} &= \left[c_j^x - c^{xx} - \xi(c_i^x - c^{xx})\right]^2 . \end{aligned} \tag{2.16}$$

On substituting all this into expression (2.4) for $\mathcal{F}$ one finds for the free energy functional per spin Φ

$$\begin{aligned} \Phi \equiv \frac{\mathcal{F}}{Nk_BT} = -\frac{1}{N}\Bigg(\sum_{\langle ij\rangle} 2K_{ij}c_{ij}^{xx} + K_{z\,ij}c_{ij}^{zz} + \sum_{i=1}^{N} Hc_i^z\Bigg) \\ + \frac{1}{N}\Bigg[\sum_{i=1}^{N}\sum_{k=1}^{2}(\mu_{i\,k}^0 + \mu_{i\,k}^2)\ln\mu_{i\,k}^0 \\ + \sum_{\langle ij\rangle}\sum_{k=1}^{4}(\lambda_{ij\,k}^0 + \lambda_{ij\,k}^2)\ln\lambda_{ij\,k}^0 \\ - \sum_{\langle ij\rangle}\sum_{k=1}^{2}(\mu_{i\,k}^0 + \mu_{i\,k}^2)\ln\mu_{i\,k}^0 + (\mu_{j\,k}^0 + \mu_{j\,k}^2)\ln\mu_{j\,k}^0\Bigg] \end{aligned} \tag{2.17}$$

where

$$K_{ij} \equiv \frac{J_{ij}}{k_BT} \qquad K_{z\,ij} \equiv \frac{J_{z\,ij}}{k_BT} \qquad H \equiv \frac{h}{k_BT} . \tag{2.18}$$

After also expanding this expression to second-order in the other 'order' parameters (like $\tilde{m}_i$), it can be separated into two terms. The first one, Φ_0, only contains the parameters associated with the disordered phase, c_{ij}^{xx}, c_{ij}^{zz}, and m_i, while the other one, Φ_2, is bilinear in the various 'order' parameters. (If one wants to consider the case $h = 0$, one should expand Φ to second-order in m_i too, and include m_i in the set of 'order' parameters.) Φ can now be written†

$$\Phi = \Phi_0 + \Phi_2 + \cdots = \Phi_0 + \mathbf{c}^{\mathrm{T}}\mathbf{M}\mathbf{c} + \cdots \tag{2.19}$$

where $\mathbf{c}$ is a vector containing all 'order' parameters, and $\mathbf{M}$ is the symmetric matrix

$$\mathbf{M}_{ij} = \left.\frac{\partial^2\Phi}{\partial c_i \partial c_j}\right|_{c=0} . \tag{2.20}$$

The matrix $\mathbf{M}$ itself only depends on the parameters of the disordered phase, c_{ij}^{xx}, c_{ij}^{zz}, and m_i. Since Φ_2 does not contain terms that are a product of 'order' parameters for different phases, the matrix $\mathbf{M}$ is block diagonal. It contains a block $\mathbf{M}^{\mathrm{AI}}$

† Note that the definition of Φ_2 is different from that in [13].

corresponding to the 'order' parameters of the antiferromagnetic Ising phase, a block $\mathbf{M}^{XY}$ for those of the x–y ordered phase, and in the case $h = 0$ a block $\mathbf{M}^{FI}$ for the ferromagnetic Ising phase.

Now the minimization of Φ in the disordered phase boils down to minimizing Φ_0, since the minimization with respect to $\mathbf{c}$ gives the equation $\mathbf{Mc} = 0$, which in this phase has the trivial solution $\mathbf{c} = 0$, i.e. all 'order' parameters are zero. In an ordered phase, on the other hand, there is also a solution for the minimization equations for Φ with some elements of $\mathbf{c}$ non-zero. The two solutions bifurcate for $\det \mathbf{M} = 0$, so this is the equation giving the phase boundary. Since $\mathbf{M}$ is block diagonal, the three different phase boundaries follow from

$$\det \mathbf{M}^P = 0 \tag{2.21}$$

with $P = \text{AI}, \text{XY}, \text{FI}$ for the antiferromagnetic Ising phase, the x–y ordered phase, and the ferromagnetic Ising phase, respectively. The procedure for finding the phase boundaries is then first to solve the minimization equations for Φ_0 for the disordered phase only, substitute the result into $\mathbf{M}$, and then to solve (2.21). In some cases, e.g. when the field h is zero, this can be done analytically, but if necessary the whole minimization can be done numerically.

3. The spatially anisotropic geometry

To apply the method described in the previous section to a specific geometry, one only needs to identify the different types of clusters, and count how often they occur in the lattice. As a first example we will consider a cubic lattice with a spatially anisotropic interaction. The lattice consists of a collection of parallel quadratic planes, and the coupling between spins that lie in the same plane is different from the coupling between spins in adjacent planes. We will take the coupling within the planes to be larger than that between planes, so one has a stack of (more or less) weakly coupled layers. By varying the ratio of the inter-layer and intra-layer couplings from zero to one, the system changes from a collection of uncoupled, two-dimensional quadratic lattices to an isotropic three-dimensional cubic lattice.

3.1. The calculation of $\mathbf{M}^P$

For this geometry the Hamiltonian (1.1) reduces to

$$\mathcal{H} = \sum_{\langle ij\rangle_\parallel} -J_\parallel(\sigma_i^x\sigma_j^x + \sigma_i^y\sigma_j^y) - J_{z\parallel}\sigma_i^z\sigma_j^z + \sum_{\langle ij\rangle_\perp} -J_\perp(\sigma_i^x\sigma_j^x + \sigma_i^y\sigma_j^y) - J_{z\perp}\sigma_i^z\sigma_j^z - \sum_{i=1}^{N} h\sigma_i^z \,. \tag{3.1}$$

The summation $\sum_{\langle ij\rangle_\parallel}$ extends over all nearest-neighbour pairs of spins inside the layers, while the sum $\sum_{\langle ij\rangle_\perp}$ runs over nearest-neighbour pairs that lie in adjacent layers. The couplings $J_\parallel$ and $J_{z\parallel}$, and $J_\perp$ and $J_{z\perp}$ are the intra-layer and inter-layer couplings, respectively.

Apart from the distinction between the sublattices a and b, all sites of the lattice are equivalent. There are, therefore, two one-spin reduced density matrices, $\rho_a^{(1)}$ and

$\rho_b^{(1)}$, and two corresponding cluster entropies, $S_a^{(1)}$ and $S_b^{(1)}$. There are also two different types of two-spin clusters, since in this geometry a cluster of two spins in the same layer is not equivalent to one of two spins in adjacent layers. Thus one has two two-spin reduced density matrices, $\rho_{\|}^{(2)}$ and $\rho_{\perp}^{(2)}$, and two cluster entropies, $S_{\|}^{(2)}$ and $S_{\perp}^{(2)}$. Consequently, one finds for the energy terms in (2.4)

$$\begin{aligned}\mathrm{Tr}(\rho\mathcal{H}) &= \sum_{i=1}^{N}\mathrm{Tr}(\rho_i^{(1)}h_i^{(1)}) + \sum_{\langle ij\rangle\|}\mathrm{Tr}(\rho_{\|}^{(2)}h_{ij}^{(2)}) + \sum_{\langle ij\rangle\perp}\mathrm{Tr}(\rho_{\perp}^{(2)}h_{ij}^{(2)}) \\ &= -N\left(4J_{\|}c_{\|}^{xx} + 2J_{z\|}c_{\|}^{zz} + 2J_{\perp}c_{\perp}^{xx} + J_{z\perp}c_{\perp}^{zz} + mh\right) \qquad (3.2)\end{aligned}$$

since out of the 6 neighbours of a particular spin 4 lie in the same layer, and 2 lie in adjacent layers. For the entropy one similarly finds

$$\begin{aligned}k_{\mathrm{B}}\mathrm{Tr}(\rho\ln\rho) &= \left(5\sum_{i=1}^{N}S_i^{(1)} - \sum_{\langle ij\rangle\|}S_{\|}^{(2)} - \sum_{\langle ij\rangle\perp}S_{\perp}^{(2)}\right) \\ &= k_{\mathrm{B}}N\Big[-\tfrac{5}{2}\sum_{q=a,b}\mathrm{Tr}(\rho_q^{(1)}\ln\rho_q^{(1)}) + 2\mathrm{Tr}(\rho_{\|}^{(2)}\ln\rho_{\|}^{(2)}) \\ &\quad + \mathrm{Tr}(\rho_{\perp}^{(2)}\ln\rho_{\perp}^{(2)})\Big]. \qquad (3.3)\end{aligned}$$

The disordered phase is described by five parameters: m, $c_{\|}^{xx}$, $c_{\|}^{zz}$, $c_{\perp}^{xx}$, and $c_{\perp}^{zz}$. The values of these parameters can be found by minimizing Φ_0, which in this case is given by

$$\begin{aligned}\Phi_0 &= -\left(4K_{\|}c_{\|}^{xx} + 2K_{z\|}c_{\|}^{zz} + 2K_{\perp}c_{\perp}^{xx} + K_{z\perp}c_{\perp}^{zz} + mH\right) \\ &\quad - 5\mathcal{P}^{(1)} + 2\mathcal{P}_{\|}^{(2)} + \mathcal{P}_{\perp}^{(2)}. \qquad (3.4)\end{aligned}$$

The contributions from the three terms in (3.3) are obtained by setting the 'order' parameters equal to zero in the eigenvalues of the density matrices. This gives

$$\begin{aligned}\mathcal{P}^{(1)} &= \tfrac{1}{2}\left(\ln(1-m^2) + m\ln\frac{1+m}{1-m}\right) - \ln 2 \\ \mathcal{P}_{\zeta}^{(2)} &= \sum_{k=1}^{4}\lambda_{\zeta k}^{0}\ln\lambda_{\zeta k}^{0} \qquad (\zeta = \|, \perp).\end{aligned} \qquad (3.5)$$

The eigenvalues $\lambda_{\zeta k}^{0}$ in the disordered phase are simply the expressions (2.13) with $c_i^x = c_j^x = m$.

Performing the minimization with respect to $c_{\zeta}^{\alpha\alpha}$, we find that the equations for $\zeta = \|$ and $\zeta = \perp$ decouple, and that they are the same apart from an overall factor,

$$\begin{aligned}\frac{\partial}{\partial c_{\zeta}^{xx}}\Phi_0 \propto 2K_{\zeta} - \frac{\partial}{\partial c_{\zeta}^{xx}}\mathcal{P}_{\zeta}^{(2)} &= 2K_{\zeta} - \tfrac{1}{2}\ln\frac{\lambda_{\zeta 2}^{0}}{\lambda_{\zeta 3}^{0}} = 0 \\ \frac{\partial}{\partial c_{\zeta}^{zz}}\Phi_0 \propto K_{z\zeta} - \frac{\partial}{\partial c_{\zeta}^{zz}}\mathcal{P}_{\zeta}^{(2)} &= K_{z\zeta} - \tfrac{1}{4}\ln\frac{\lambda_{\zeta 1}^{0}\lambda_{\zeta 4}^{0}}{\lambda_{\zeta 2}^{0}\lambda_{\zeta 3}^{0}} = 0.\end{aligned} \qquad (3.6)$$

Equations (3.6) can be solved, and the result is the same as that for an infinite isotropic lattice [13]

$$c_\zeta^{zz} = \frac{\sigma_\zeta + \theta_\zeta - 2\left(\sigma_\zeta\theta_\zeta + m^2(\theta_\zeta^2 - \sigma_\zeta\theta_\zeta)\right)^{1/2}}{\sigma_\zeta - \theta_\zeta} \qquad (3.7)$$

$$c_\zeta^{xx} = \tfrac{1}{2}(1 - c_\zeta^{zz})\tanh(2K_\zeta)$$

where

$$\sigma_\zeta \equiv e^{4K_{z\zeta}} \qquad \theta_\zeta \equiv \cosh^2(2K_\zeta)\,. \qquad (3.8)$$

The result of minimizing in m is

$$\frac{\partial}{\partial m}\Phi_0 = -H + \frac{\partial}{\partial m}\left(-5\mathcal{P}^{(1)} + 2\mathcal{P}_\parallel^{(2)} + \mathcal{P}_\perp^{(2)}\right)$$
$$= -H - \tfrac{5}{2}\ln\frac{1+m}{1-m} + \ln\frac{1+2m+c_\parallel^{zz}}{1-2m+c_\parallel^{zz}} + \tfrac{1}{2}\ln\frac{1+2m+c_\perp^{zz}}{1-2m+c_\perp^{zz}} = 0\,. \qquad (3.9)$$

This equation should be solved, together with (3.7), to give m as a function of H, or, if m is considered as an externally imposed parameter, it gives the field H required to produce that value of m.

The second-order term Φ_2 is

$$\Phi_2 = c^{\mathrm{T}}\mathbf{M}c \qquad (3.10)$$

where the vector $c^{\mathrm{T}} = (\bar{m}, c^x, c_\parallel^{xz}, c_\perp^{xz})$ contains the 'order' parameters. The matrix $\mathbf{M}$ is a block diagonal matrix consisting of a 1 by 1 block $\mathbf{M}^{\mathrm{AI}}$, giving the coefficient of the term quadratic in $\bar{m}$, and a 3 by 3 block $\mathbf{M}^{\mathrm{XY}}$ coupling the other three 'order' parameters, $(c^x, c_\parallel^{xz}, c_\perp^{xz})$

$$\mathbf{M}^{\mathrm{AI}} = -\frac{5}{1-m^2} + \frac{1}{c_\parallel^{xx}}\ln\frac{\lambda_{\parallel 2}^0}{\lambda_{\parallel 3}^0} + \frac{1}{2c_\perp^{xx}}\ln\frac{\lambda_{\perp 2}^0}{\lambda_{\perp 3}^0} \qquad (3.11)$$

and

$$M_{1,1}^{\mathrm{XY}} = -\frac{5}{m}\ln\frac{1+m}{1-m} + 4(\ell_{12}^\parallel + \ell_{24}^\parallel) + 2(\ell_{12}^\perp + \ell_{24}^\perp)$$
$$M_{1,2}^{\mathrm{XY}} = M_{2,1}^{\mathrm{XY}} = 4(\ell_{12}^\parallel - \ell_{24}^\parallel)$$
$$M_{1,3}^{\mathrm{XY}} = M_{3,1}^{\mathrm{XY}} = 2(\ell_{12}^\perp - \ell_{24}^\perp) \qquad (3.12)$$
$$M_{2,2}^{\mathrm{XY}} = 4(\ell_{12}^\parallel + \ell_{24}^\parallel)$$
$$M_{2,3}^{\mathrm{XY}} = M_{3,2}^{\mathrm{XY}} = 0$$
$$M_{3,3}^{\mathrm{XY}} = 2(\ell_{12}^\perp + \ell_{24}^\perp)$$

where

$$\ell^{\zeta}_{km} \equiv \frac{\ln(\lambda^0_{\zeta k}/\lambda^0_{\zeta m})}{4(\lambda^0_{\zeta k} - \lambda^0_{\zeta m})} \qquad (\zeta = \|, \perp)\,. \tag{3.13}$$

If one wants to consider the case $h = 0$, m must be set equal to zero in Φ_0, and included in the vector c. M will then also contain a 1 by 1 block M^{FI} giving the coefficient of m^2, which is equal to

$$\mathsf{M}^{\mathrm{FI}} = -5 + \frac{4}{1 + c^{zz}_{\|}} + \frac{2}{1 + c^{zz}_{\perp}}\,. \tag{3.14}$$

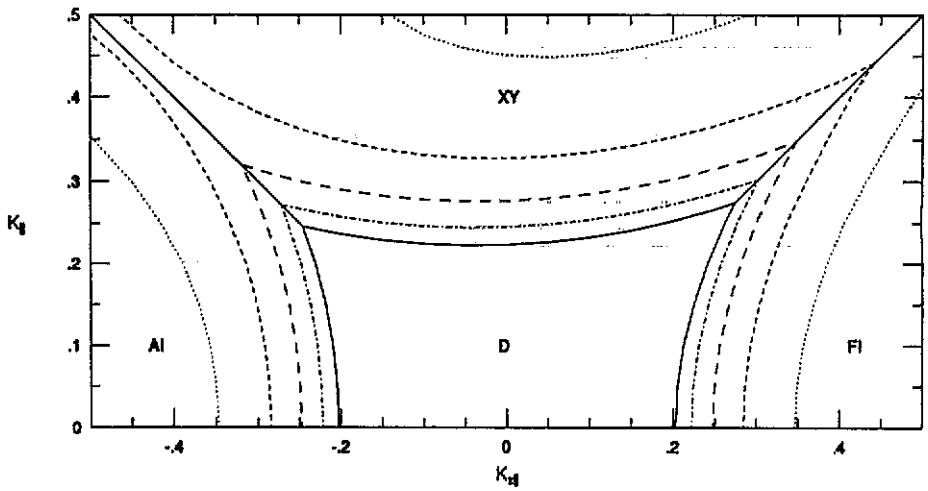

Figure 1. The phase diagram for the spatially anisotropic geometry. The phase boundaries have been drawn for $\eta = 0$ (·····), $1/4$ (– – –), $1/2$ (— — —), $3/4$ (— · —), and 1 (——). The magnetic field H is zero.

3.2. Results

The phase diagram we obtain for this geometry is shown in figure 1 for different values of the spatial anisotropy η, and the magnetic field H equal to zero. We will always take the anisotropy in spin space equal for the intra-layer and inter-layer couplings, so that for the spatial anisotropy we have $\eta = K_\perp/K_\| = K_{z\perp}/K_{z\|}$. The two-dimensional case is recovered for $\eta = 0$, and the three-dimensional one for $\eta = 1$. The other three values, $\eta = 1/4, 1/2, 3/4$, interpolate between these two. The structure of the phase diagrams is roughly as follows: at high temperatures (around $K_\| = K_{z\|} = 0$) the system is in the disordered phase (D). The ordered phases one finds at lower temperature are the ferromagnetic Ising phase (FI) for $K_{z\|} > K_\| > 0$, the antiferromagnetic Ising phase (AI) for $-K_{z\|} > K_\| > 0$, and the x–y ordered phase (XY) for $K_\| > |K_{z\|}|$. The boundaries between these three phases and the disordered phase follow from the equations $\det \mathsf{M}^P = 0$. For

$H = 0$ the Ising phases are separated from the XY phase by the lines $K_{\|} = K_{z\|}$ and $K_{\|} = -K_{z\|}$.

As η is increased from zero to one, the disordered region (D) shrinks, the phase boundaries moving towards lower values of K (higher temperatures). The general shape of the disordered region changes little; for the Ising, XY, antiferromagnetic and ferromagnetic Heisenberg models one has $K_c^{\mathrm{I}} < K_c^{\mathrm{XY}} < K_c^{\mathrm{AH}} < K_c^{\mathrm{FH}}$ for most values of η. Two qualitative changes take place. First, the critical coupling of the ferromagnetic Heisenberg model, which is infinite in two dimensions, becomes finite as soon as the inter-layer coupling is turned on. This is consistent with the fact that the lower critical dimension of this model is 2. Second, the antiferromagnetic Heisenberg model does not exhibit a phase transition for $\eta \lesssim 1/4$. This is related to the fact that the cluster variation method, and similar approximations, predict a spurious phase transition at low temperatures [12, 13, 14]. As the temperature is lowered, both the AI and XY order disappear, and the system remains disordered down to $T = 0$. For low dimensions, and in this case for small η, this artifact of the approximation interferes with the phase transition at higher temperature. So, unfortunately, no conclusions can be drawn about the behaviour of the antiferromagnetic Heisenberg model near two dimensions, which is of great interest in connection with theories of high-T_c superconductors. For $\eta \gtrsim 1/2$, this unphysical transition takes place at such a low temperature that it is clearly separated from the physical ones, and the phase diagram is barely influenced by it. In fact, for the three-dimensional isotropic case ($\eta = 1$), it turns out that the accuracy is quite good when compared to high temperature series expansions.

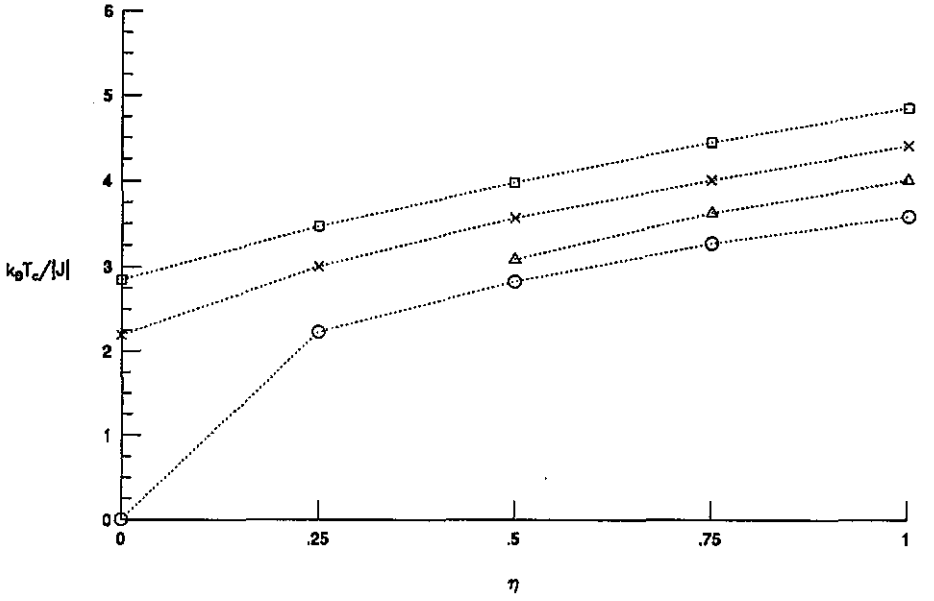

Figure 2. The critical temperature for the spatially anisotropic geometry, as a function of η. The values of $k_BT_c/|J|$ have been plotted for some special cases of the XXZ Hamiltonian, viz. Ising (□), XY (×), antiferromagnetic Heisenberg (△), and ferromagnetic Heisenberg (○) interactions. The lines have only been drawn to guide the eye.

In order to show the change of T_c from its two-dimensional value to that for three

dimensions, figure 2 shows a plot of $k_B T_c/|J| = 1/|K|$ versus the spatial anisotropy η. The values given are for some special cases of the Hamiltonian (3.1), namely the Ising, XY, antiferromagnetic and ferromagnetic Heisenberg models.

4. The slab geometry

Another geometry that shows a cross-over from two to three dimensions is that of a slab consisting of a finite number, n, of simple quadratic layers. We will take the coupling constants equal in all directions, and by letting n run from 1 to ∞ the system changes from a two-dimensional simple quadratic lattice to a three-dimensional cubic lattice. The Hamiltonian is basically given by (1.1), with $J_{ij} = J$, $J_{z\,ij} = J_z$, a homogeneous magnetic field h, and the sum running over n layers containing N/n spins each. The top and bottom layers have free boundary conditions. A similar calculation for the Ising model can be found in [15].

4.1. The calculation of $\mathbf{M}^P$

Since the slab has only a finite thickness, there is no translation symmetry in the direction perpendicular to its surface. Therefore all n layers (which we will indicate by an index r running from 1 to n) are different, except for a reflection symmetry in the middle plane of the slab, so that layers r and $n+1-r$ are equivalent. Quantities that refer to one layer only, like the one-spin cluster entropies and the cluster entropy for two spins in the same layer, will be given an index r indicating the layer they refer to. Quantities that refer to two adjacent layers, like the cluster entropy for two spins in different layers, will also be given an index r, now indicating that they refer to layers r and $r+1$. For these quantities the reflection symmetry means that those labelled r and $n-r$ are equivalent. The two sublattices necessary for the description of an antiferromagnetically ordered state are defined on the cubic lattice, so that a site on sublattice a in layer r is adjacent to sites on sublattice b in layers $r-1$, $r+1$, and r.

For each layer r we consequently have two one-spin cluster entropies, $S_{ra}^{(1)}$ and $S_{rb}^{(1)}$, and one cluster entropy for two spins within the layer, $S_{r\parallel}^{(2)}$. There are two cluster entropies for spins in different layers, $S_{r\perp a}^{(2)}$ where the spin in layer r is on the a sublattice and the one in layer $r+1$ on the b sublattice, and $S_{r\perp b}^{(2)}$, where this is the other way round.

For the free energy functional Φ this leads to the expression

$$
\begin{aligned}
n\Phi = \sum_{r=1}^{n} \Big[-4\Big(K c_{r\parallel}^{xx} + \frac{K_z}{2} c_{r\parallel}^{zz}\Big) - H m_r + \frac{1}{k_B}\Big(\tfrac{5}{2}(S_{ra}^{(1)} + S_{rb}^{(1)}) - 2S_{r\parallel}^{(2)}\Big)\Big] \\
+ \sum_{r=1}^{n-1} \sum_{q=a,b} \Big[-\Big(K c_{r\perp q}^{xx} + \frac{K_z}{2} c_{r\perp q}^{zz}\Big) - \frac{1}{2k_B} S_{r\perp q}^{(2)}\Big] \\
- \frac{1}{2k_B}(S_{1a}^{(1)} + S_{1b}^{(1)} + S_{na}^{(1)} + S_{nb}^{(1)}) \,. \qquad (4.1)
\end{aligned}
$$

The last term is a correction due to the fact that the top and bottom layers have only one neighbouring layer. In the disordered phase the non-zero parameters are m_r,

$c_{r\parallel}^{xx}$, and $c_{r\parallel}^{zz}$ for every layer, and $c_{r\perp}^{xx}$ and $c_{r\perp}^{zz}$ for every pair of adjacent layers—$c_{r\perp}^{\alpha\alpha} = (c_{r\perp a}^{\alpha\alpha} + c_{r\perp b}^{\alpha\alpha})/2$. Hence we find for Φ_0

$$n\Phi_0 = \sum_{r=1}^{n}\left[-4\left(Kc_{r\parallel}^{xx} + \frac{K_z}{2}c_{r\parallel}^{zz}\right) - Hm_r - 5\mathcal{P}_r^{(1)} + 2\mathcal{P}_{r\parallel}^{(2)}\right]$$
$$+ \sum_{r=1}^{n-1}\left[-2\left(Kc_{r\perp}^{xx} + \frac{K_z}{2}c_{r\perp}^{zz}\right) + \mathcal{P}_{r\perp}^{(2)}\right] + \mathcal{P}_1^{(1)} + \mathcal{P}_n^{(1)} \tag{4.2}$$

where

$$\mathcal{P}_r^{(1)} = \tfrac{1}{2}\left(\ln(1-m_r^2) + m_r \ln\frac{1+m_r}{1-m_r}\right) - \ln 2$$
$$\mathcal{P}_{r\zeta}^{(2)} = \sum_{k=1}^{4}\lambda_{r\zeta\,k}^{0}\ln\lambda_{r\zeta\,k}^{0} \qquad (\zeta = \parallel, \perp)\,. \tag{4.3}$$

In the disordered phase, the eigenvalues $\lambda_{r\parallel\,k}^{0}$, where both spins in the cluster are in layer r, are obtained from (2.13) by setting $c_i^z = c_j^z = m_r$. For two spins in adjacent layers, r and $r+1$, we get $\lambda_{r\perp\,k}^{0}$ from (2.13) by setting $c_i^z = m_r$ and $c_j^z = m_{r+1}$. The presence of the magnetization profile m_r prevents us from treating the disordered phase analytically, so the minimization in the presence of a field H has to be done numerically. If H is zero, however, and consequently there is no magnetization, an analytical treatment *is* possible. This will be done in the following section.

The second-order term Φ_2 is again of the form $\Phi_2 = c^{\mathrm{T}}\mathsf{M}c$, where now $c^{\mathrm{T}} = (\bar{m}_r, \delta_r^{xx}, \delta_r^{zz}, c_r^x, c_{r\parallel}^{xz}, c_{r\perp}^{xz}, c_{r\perp}^{zx})$ contains a large number of 'order' parameters. For the antiferromagnetic Ising phase there is the staggered magnetization $\bar{m}_r = (c_{ra}^z - c_{rb}^z)/2$ for each layer. In addition, the quantities $\delta_r^{\alpha\alpha} = (c_{r\perp a}^{\alpha\alpha} - c_{r\perp b}^{\alpha\alpha})/2$ are also non-zero when the two sublattices a and b are different, which gives rise to these new 'order' parameters. For the x–y ordered phase c contains the magnetization in the x–y plane, c_r^x, the intra-layer correlation $c_{r\parallel}^{xz}$, and the two inter-layer correlations $c_{r\perp}^{xz}$ and $c_{r\perp}^{zx}$. For the case $h = 0$ the parameters m_r must be set equal to zero in Φ_0, and included in c as the 'order' parameters for the ferromagnetic Ising phase. The structure of the matrices M^P is given in the appendix.

4.2. The case $H = 0$

In general the determination of the phase boundaries for the slab geometry must be done numerically, but if $H = 0$ one can proceed analytically, as we will first do for the x–y phase boundary. In this case the description of the disordered phase simplifies due to the fact that there is no magnetization profile m_r. For $H = 0$ and $m_r = 0$, equation (4.2) becomes

$$n\Phi_0 = \sum_{r=1}^{n} f_r^{\parallel} + \sum_{r=1}^{n-1} f_r^{\perp} - 2\ln 2 \tag{4.4}$$

with

$$f_r^{\parallel}(c_{r\parallel}^{xx}, c_{r\parallel}^{zz}) = -4(Kc_{r\parallel}^{xx} + \tfrac{1}{2}K_z c_{r\parallel}^{zz}) - 5\ln 2 + 2\mathcal{P}_{r\parallel}^{(2)}$$
$$f_r^{\perp}(c_{r\perp}^{xx}, c_{r\perp}^{zz}) = -2(Kc_{r\perp}^{xx} + \tfrac{1}{2}K_z c_{r\perp}^{zz}) + \mathcal{P}_{r\perp}^{(2)}. \tag{4.5}$$

Now minimizing Φ_0 with respect to a parameter $c_{r\zeta}^{\alpha\alpha}$ of the disordered phase gives

$$\frac{\partial}{\partial c_{r\zeta}^{\alpha\alpha}} n\Phi_0 = \frac{\partial}{\partial c_{r\zeta}^{\alpha\alpha}} f_r^{\zeta} = 0 \qquad (\alpha = x, z) \tag{4.6}$$

because there is only one term in (4.4) containing the parameter $c_{r\zeta}^{\alpha\alpha}$. Moreover, apart from an overall factor of 2, the dependence of f_r^{ζ} on $c_{r\zeta}^{\alpha\alpha}$ is the same for any r and ζ. So, as in (3.6), we find for all r and ζ

$$2K - \frac{\partial}{\partial c_{r\zeta}^{xx}}\mathcal{P}_{r\zeta}^{(2)} = 2K - \tfrac{1}{2}\ln\frac{\lambda_{r\zeta 2}^0}{\lambda_{r\zeta 3}^0} = 0$$
$$K_z - \frac{\partial}{\partial c_{r\zeta}^{zz}}\mathcal{P}_{r\zeta}^{(2)} = K_z - \tfrac{1}{4}\ln\frac{(\lambda_{r\zeta 1}^0)^2}{\lambda_{r\zeta 2}^0\lambda_{r\zeta 3}^0} = 0. \tag{4.7}$$

The expressions $\mathcal{P}_{r\zeta}^{(2)}$ only depend, through (4.3) and (2.13), on $c_{r\zeta}^{xx}$ and $c_{r\zeta}^{zz}$. The equations (4.7), that determine the correlations $c_{r\zeta}^{\alpha\alpha}$, can be solved independently of r and ζ. The solutions one finds are again just the same as in the case of an infinite lattice, namely

$$c_{r\zeta}^{zz} \equiv c^{zz} = \frac{e^{2K_z} - \cosh 2K}{e^{2K_z} + \cosh 2K} \tag{4.8}$$

$$c_{r\zeta}^{xx} \equiv c^{xx} = \frac{\sinh 2K}{e^{2K_z} + \cosh 2K}. \tag{4.9}$$

To find the phase boundary, we calculate the second-order term Φ_2 of the free energy functional,

$$n\Phi_2 = \sum_{r=1}^{n} -5\mathcal{Q}_r^{(1)} + 2\mathcal{Q}_{r\parallel}^{(2)} + \sum_{r=1}^{n-1}\mathcal{Q}_{r\perp}^{(2)} + \mathcal{Q}_1^{(1)} + \mathcal{Q}_n^{(1)} \tag{4.10}$$

with

$$\mathcal{Q}_r^{(1)} = c_r^{x\,2}$$
$$\mathcal{Q}_{r\zeta}^{(2)} = \sum_{k=1}^{4}\lambda_{r\zeta k}^2 \ln\lambda_{r\zeta k}^0 = \begin{cases} 4uc_r^{x\,2} & (\zeta = \parallel) \\ u(c_r^x + c_{r+1}^x)^2 + v(c_r^x - c_{r+1}^x)^2 & (\zeta = \perp) \end{cases} \tag{4.11}$$

and, using equation (4.7),

$$u = \frac{K_z - K}{2(c^{zz} - c^{xx})}$$
$$v = \frac{K_z + K}{2(c^{zz} + c^{xx})}. \tag{4.12}$$

Minimizing Φ_2 we find the system of equations $\partial n\Phi_2/\partial c_r^x = 0$, which turns out to be

$$\begin{aligned} &b_1 c_1^x + a c_2^x = 0 \\ &a c_{r-1}^x + b c_r^x + a c_{r+1}^x = 0 \qquad (1 < r < n) \\ &a c_{n-1}^x + b_1 c_n^x = 0 \end{aligned} \tag{4.13}$$

with

$$\begin{aligned} a &= \frac{K_z - K}{c^{zz} - c^{xx}} - \frac{K_z + K}{c^{zz} + c^{xx}} \\ b &= 10\frac{K_z - K}{c^{zz} - c^{xx}} + 2\frac{K_z + K}{c^{zz} + c^{xx}} - 10 \\ b_1 &= 9\frac{K_z - K}{c^{zz} - c^{xx}} + \frac{K_z + K}{c^{zz} + c^{xx}} - 8 . \end{aligned} \tag{4.14}$$

The system (4.13) admits solutions of the form $c_r^x = \alpha y^r$. From the equation for $1 < r < n$ we find

$$a(y^{r-1} + y^{r+1}) + by^r = 0 \tag{4.15}$$

or

$$y_\pm = \frac{-b \pm \sqrt{b^2 - 4a^2}}{2a} \tag{4.16}$$

and

$$c_r^x = \alpha y_+^r + \beta y_-^r . \tag{4.17}$$

Substituting (4.17) into the equations for the boundary layers then gives

$$\begin{aligned} &(b_1 y_+ + a y_+^2)\alpha + (b_1 y_- + a y_-^2)\beta = 0 \\ &(b_1 y_+^n + a y_+^{n-1})\alpha + (b_1 y_+^n + a y_+^{n-1})\beta = 0 . \end{aligned} \tag{4.18}$$

The trivial solution $\alpha = \beta = 0$ gives the disordered phase, where the magnetization is zero; at the point where the determinant of the coefficients vanishes, the solution bifurcates, and this signals the transition into the x–y ordered phase.

It follows from (4.15) that $y_+ y_- = 1$, and for $b^2 > 4a^2$, $y_\pm$ are real. For $b^2 < 4a^2$ they are complex conjugates, so $y_+ = e^{-i\phi}$, $y_- = e^{i\phi}$. For high temperatures one finds that $b^2 > 4a^2$, giving real $y_\pm$. Lowering T, one comes to a point where $b^2 = 4a^2$, and $y_+ = y_- = 1$. This happens at $T_c(\infty)$, the critical temperature for the infinite cubic lattice. Due to translation invariance, the spontaneous magnetization of this system is homogeneous. The equation $b = -2a$ is equivalent to

$$6(K_z - K)\frac{e^{2K_z} + \cosh 2K}{e^{2K_z} - e^{2K}} = 5 \tag{4.19}$$

which is indeed the equation for the phase boundary of a system with coordination number $z = 6$ as found previously [13]. At $T_c(\infty)$ a layer of finite width is still disordered, since the bifurcation of the solution of (4.18) has not yet taken place.

Below $T_c(\infty)$, we have $y_+ = e^{-i\phi}$ and $y_- = e^{i\phi}$, so $c_r^x = \alpha e^{-ir\phi} + \beta e^{ir\phi}$, with $\tan\phi = \sqrt{4a^2/b^2 - 1}$. The determinant of (4.18) then gives

$$(b_1 + ae^{-i\phi})^2 = e^{-2(n-1)i\phi}(b_1 + ae^{i\phi})^2 . \tag{4.20}$$

The solution with $\phi = 0$ corresponds to the bulk transition temperature $T_c(\infty)$, and does not indicate a phase transition in the finite slab. This transition corresponds to the first non-zero value of ϕ satisfying (4.20), which is a solution of

$$b_1 + ae^{-i\phi} = -e^{-(n-1)i\phi}(b_1 + ae^{i\phi}) . \tag{4.21}$$

Hence we find that the solution of (4.21) corresponding to the smallest non-zero value for ϕ gives the critical temperature $T_c(n)$ of an n-layer slab. In the limit of large n, the value of ϕ at $T_c(n)$ approaches its value for the infinite lattice, $\phi = 0$ at $T_c(\infty)$. By expanding (4.21) for small ϕ and large n we find that ϕ goes to zero as $\phi \approx \pi/(n+q)$, with q given by $q = -(3a + b_1)/(a + b_1)$ calculated at $T_c(\infty)$. It can be shown that $q \geqslant 0$ for all K and K_z.

In addition to the critical temperature, we also find the shape of the order parameter profile c_r^x at the onset of the ordered phase. The normalization is determined by the higher-order terms of Φ, but since *at* $T_c(n)$ the amplitude is zero anyway, the shape of the profile is the only quantity of interest. We first observe that, in order to have a real-valued magnetization, we must have $\beta = \alpha^*$, so

$$c_r^x = |\alpha|(e^{-i(r\phi+\phi_0)} + e^{i(r\phi+\phi_0)}) = 2|\alpha|\cos(r\phi + \phi_0) . \tag{4.22}$$

The angle ϕ_0 can easily be found from the symmetry requirement that $c_r^x = c_{n+1-r}^x$, which gives $\phi_0 \equiv \theta - \pi/2 = -(n+1)\phi/2$, and

$$c_r^x = 2|\alpha|\sin(r\phi + \theta) . \tag{4.23}$$

Exactly the same treatment can be applied to the ferromagnetic and antiferromagnetic Ising phases; the only difference lies in the expressions for a, b, and b_1. For the ferromagnetic Ising phase they are

$$\begin{aligned} a &= \frac{1}{1 + c^{zz}} - \frac{K}{c^{xx}} \\ b &= \frac{10}{1 + c^{zz}} + 2\frac{K}{c^{xx}} - 10 \\ b_1 &= \frac{9}{1 + c^{zz}} + \frac{K}{c^{xx}} - 8 \end{aligned} \tag{4.24}$$

and for the antiferromagnetic Ising phase

$$\begin{aligned} a &= \frac{K}{c^{xx}} - \frac{1}{1 + c^{zz}} \\ b &= 10\frac{K}{c^{xx}} + \frac{2}{1 + c^{zz}} - 10 \\ b_1 &= 9\frac{K}{c^{xx}} + \frac{1}{1 + c^{zz}} - 8 . \end{aligned} \tag{4.25}$$

Using equation (4.21) combined with (4.15), (4.24) and (4.25) we can construct the phase diagram for $H = 0$.

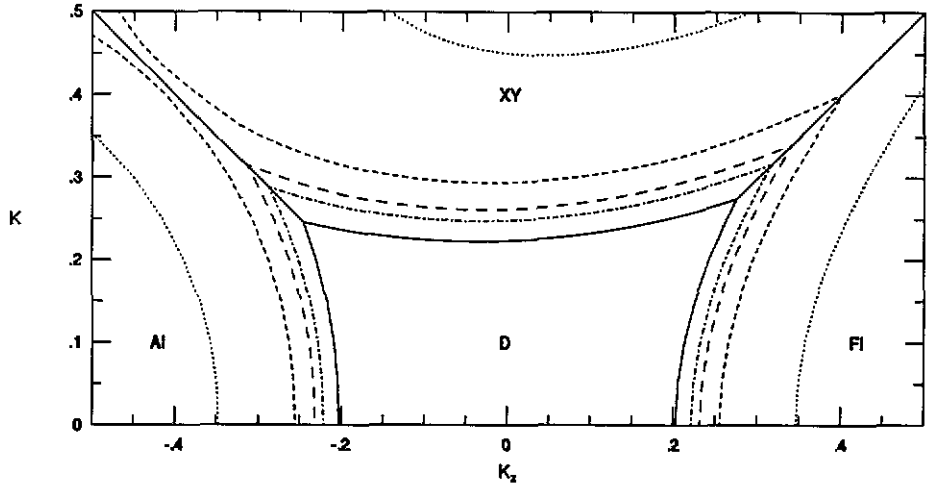

Figure 3. The phase diagram for the slab geometry. Phase boundaries are given for $n = 1$ (·····), 2 (– – –), 3 (— — —), 4 (— · —), and ∞ (——). The magnetic field H is zero.

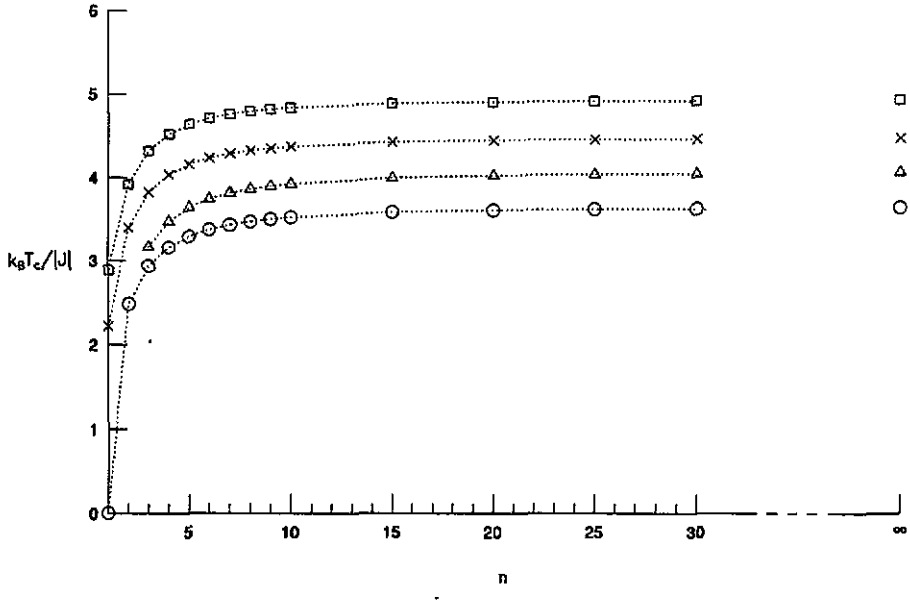

Figure 4. The critical temperature for the slab geometry for various values of n. The values of $k_BT_c/|J|$ have been plotted for some special cases of the XXZ Hamiltonian, viz. Ising (□), XY (×), antiferromagnetic Heisenberg (△), and ferromagnetic Heisenberg (○) interactions. The lines are guides for the eye.

4.3. Results

The phase diagram we find for the slab geometry is shown in figure 3 for $n = 1,2,3,4$, and ∞ and $H = 0$. For the two- and three-dimensional cases $n = 1$ and $n = \infty$ they are of course equal to the results for the infinite lattices with

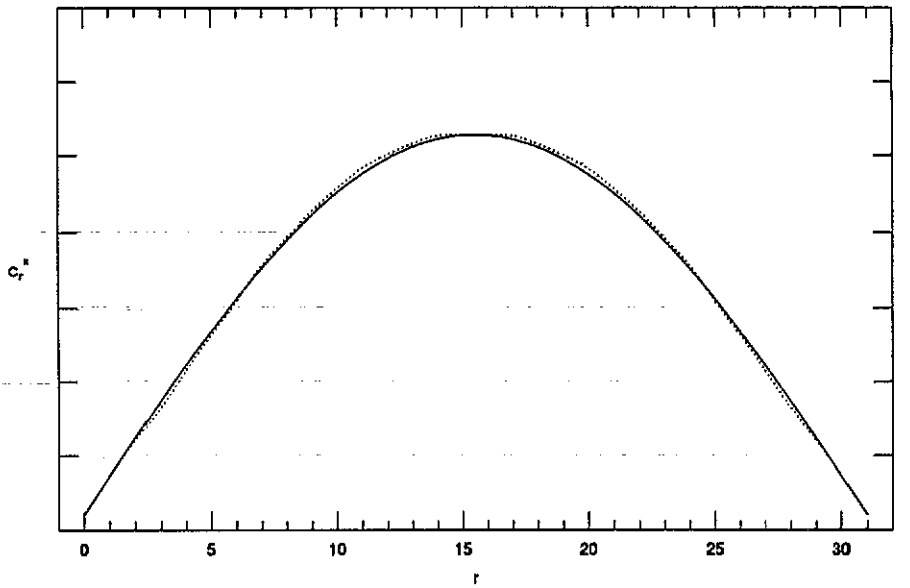

Figure 5. The order parameter profile c_r^x near T_c in a 30-layer XY slab ($K_z = 0$). For $n = 30$, the critical coupling is $K_c = 0.2243$, giving $\phi = 0.09873$ and $\theta = 0.04045$. The solid line shows $\sin(r\phi + \theta)$, scaled to match the result of a numerical minimization slightly below T_c (at $K = 0.2244$), which is given by the dotted curve.

coordination number $z = 4$ and 6, respectively, while the double layer corresponds to the case $z = 5$. The basic features of the phase diagram are the same as in section 3, with in this case the unphysical gap around $K_{z\parallel} = -K_{\parallel}$ disappearing for $n > 2$. Figure 4 again displays the behaviour of T_c when going from two to three dimensions.

For this geometry we also calculated the order parameter profile in the layer. In particular for the x–y ordered phase this is of interest, since the order parameter c_r^x (indicating off-diagonal long-range order) corresponds, in the pseudo-spin formulation of the quantum lattice gas [1], to the superfluid condensate wavefunction. It was shown in the previous section that the shape of the order parameter profile at T_c is given by $c_r^x \propto \sin(r\phi + \theta)$. In figure 5 we show the profile for the XY model in a slab of $n = 30$ layers. The critical coupling for this thickness is $K_c = 0.2243$, which corresponds to $\phi = 0.09873$, and $\theta = 0.04045$. As a comparison we have also drawn the result of numerically minimizing the full free energy functional Φ at a coupling slightly below T_c, $K = 0.2244$. The plots have been scaled so as to coincide at their maxima. Obviously the approximations made in section 4.2 hold in a small temperature range below T_c. For temperatures further below T_c, the magnetization c_r^x starts to saturate in the interior of the slab, and since this behaviour is governed by the higher-order terms in Φ the order parameter profile is no longer sinusoidal.

Some conclusions we can draw from the behaviour of c_r^x near T_c are, first, that all order parameters become non-zero simultaneously at the same temperature, so there is no separate surface transition. Second, the order parameter drops almost to zero at the slab boundary; in fact the profile goes through zero at $r_0 = (n + 1)/2 - \pi/2\phi$, which is immediately outside the slab. In the limit $n \to \infty$ we find

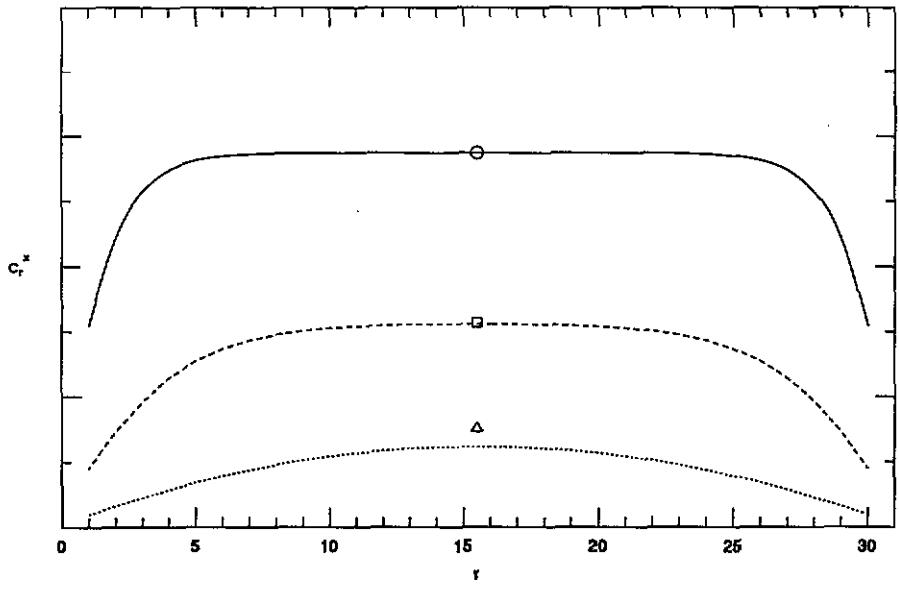

Figure 6. The order parameter profile c_r^x in a 30-layer XY slab for $K = 0.225$ (·····), $K = 0.23$ (– – –), and $K = 0.25$ (——). The critical coupling for $n = 30$ is $K_c = 0.2243$. Also plotted are the values of c_r^x in a three-dimensional lattice at the same coupling strengths (open symbols).

that $r_0 = (1 - q)/2 < 1/2$. This supports a proposition that was made recently [16], that the use of Dirichlet boundary conditions in finite-size scaling theory would be fairly realistic.

Further away from T_c, we observe that there are two effects that suppress the value of the order parameter in a layer with respect to its value in a three-dimensional lattice. For any temperature, its value will be lower in the outer layers, because of the proximity of the free boundary layer. Second, for temperatures just below T_c, the order parameter will be smaller than its three-dimensional value over the whole width of the slab, because T_c for the three-dimensional system is higher. For low enough temperatures, the magnetization takes on its three-dimensional value in the inner layers of the slab. The order parameter profile for a 30-layer slab is plotted in figure 6 for various values of K for the XY model ($K_z = 0$).

5. Discussion

To examine the merits of the cluster variation method applied to these spin models, we will compare its results with those of other approaches. We first examine the Ising transition, since the Ising model is both the simplest and the most intensively studied model described by a Hamiltonian of the form (1.1). The Ising model is known to have ordered phases with a non-zero magnetization in two and three dimensions, and in both dimensions the cluster variation estimate of T_c is considerably better than that of the mean-field approximation. Hence one would expect its result to be an improvement for the slab geometry, too. This is indeed the case, as is shown in

Table 1. The critical temperature for an Ising model ($K = 0$) slab consisting of n layers. Listed are the mean-field estimate $k_B T_c/J_z = 6 - 2/n$, the result of the two-spin cluster variation method, and the series expansion result of Capehart and Fisher [17].

	$k_B T_c/J_z$		
n	Mean-field	CVM	Series
1	4	2.89	2.27
2	5	3.92	3.23
3	5.33	4.32	3.65
4	5.5	4.52	3.88
5	5.6	4.64	4.03
6	5.67	4.71	4.14
7	5.71	4.76	4.21
∞	6	4.93	4.51

table 1, where we compare the results of these two approximations with those of series expansion techniques [17] for the pure Ising case $K = 0$. Similarly, for the spatially anisotropic geometry one would expect the cluster variation result to be an improvement over the mean-field estimate $k_B T_c/J_{\| z} = 4 + 2\eta$. Thus the Ising transition seems to confirm the pattern one usually finds for classical models: the two-spin cluster variation method overestimates T_c, but much less than the mean-field approximation. In turn, the cluster variation result can be expected to improve when one uses larger clusters. Also, as long as the Hamiltonian is Ising-like ($K_z > K \geqslant 0$), there is no unphysical transition back to the disordered state at low temperature.

The situation for the x–y transition is more complicated. For the slab geometry one expects a transition to a phase that does not have a magnetization, since it is known that such a phase cannot exist at $T \neq 0$ in a finite slab [18, 19]. This phase might have topological order à la Kosterlitz–Thouless [20]. For thick slabs the transition should cross over to a three-dimensional x–y transition. For the anisotropic geometry, on the other hand, a three-dimensional x–y transition is expected, only crossing over to a two-dimensional transition in the limit of uncoupled layers. The cluster variation method is not capable of producing a topological phase transition in these situations, and yields, as a refined mean-field method, transitions to an x–y phase with a non-zero magnetization. Only the location of the critical temperature can be meaningfully extracted from the cluster variation method. As it agrees reasonably for the pure XY model ($K_z = 0$), we may expect that in the general case $K_z \neq 0$ it also gives a good description of the phase boundary. The fact that the behaviour of T_c as a function of n is qualitatively similar to that for the Ising model is confirmed by renormalization group studies [21].

The situation near the Heisenberg model ($K_z = \pm K$) is particularly delicate. In the slab geometry, being basically two-dimensional, the transition point should diverge to $K_c = \infty$ for all slabs of a finite thickness. In the anisotropic geometry K_c stays finite for all anisotropies except for the case of uncoupled layers. To a certain extent the cluster variation method shows this picture for the ferromagnetic Heisenberg model. It gives a transition temperature $T = 0$ for the two-dimensional case, but finite transition temperatures in all other cases. It gives an increase of K_c for finite layers near the Heisenberg model, but fails to produce the divergence of K_c (or $T_c = 0$).

For the antiferromagnetic Heisenberg model the picture is similar but blurred by

Table 2. The results of the cluster variation method compared with those of the mean field approximation and of series expansion techniques [22]. Shown are the critical couplings for the Ising, XY, antiferromagnetic Heisenberg and ferromagnetic Heisenberg models, on a simple quadratic ($z = 4$) and a simple cubic ($z = 6$) lattice.

	Simple quadratic			Simple Cubic		
	Mean-field	CVM	Series	Mean-field	CVM	Series
I	0.25	0.347	0.441	0.167	0.203	0.222
XY	0.25	0.451	0.635	0.167	0.224	0.248
AH	0.25	—	—	0.167	0.246	0.260
FH	0.25	∞	∞	0.167	0.275	0.298

the interference of the spurious disordered phase at $T = 0$. The fact that for layer thicknesses below $n = 3$ the transition temperature drops to zero cannot be seen as a virtue of the cluster variation method, since it gives a similar behaviour for sufficiently anisotropic geometries. Incorporation of long wavelength fluctuations is an essential ingredient to improve the phase diagram at points where higher symmetries of the model drive the phase transition to $T = 0$.

A further comparison with series expansion results [22] is shown in table 2 for the two- and three-dimensional infinite lattice. In all cases the cluster variation method gives a considerable improvement over the mean-field result. Also, whereas the mean-field approximation gives the same value of K_c for all models listed in table 2, the cluster variation method has $K_c^{\mathrm{I}} < K_c^{\mathrm{XY}} < K_c^{\mathrm{AH}} < K_c^{\mathrm{FH}}$, in accordance with the series results. We may conclude that while the cluster variation method does not always give a good description of the phase transition, its estimate for the critical temperature is in general quite good. Especially in cases where it is not feasible to examine the whole phase diagram by more sophisticated methods, it is a useful tool.

Acknowledgments

The authors thank Dr G An for many useful discussions. Part of this research was supported by the 'Stichting voor Fundamenteel Onderzoek der Materie' (FOM) which is financially supported by the 'Stichting Nederlands Wetenschappelijk Onderzoek' (NWO).

Appendix

In this appendix we give the structure of the matrices M^P for the slab geometry described in section 4. Due to the reflection symmetry there are w different layers in an n-layer slab, with $w = n/2$ for even n, and $w = (n+1)/2$ for odd n. Quantities that pertain only to one layer will, therefore, give rise to w independent 'order' parameters, while the exact number of 'order' parameters for quantities that concern two layers depends on n being odd or even, and also on the effect of the reflection symmetry on these 'order' parameters. The matrices M^P are always symmetric, $M^P_{i,j} = M^P_{j,i}$. The elements that are not given below, and that cannot be obtained from the elements given below by using this symmetry are all zero. As was already pointed out in section 4, for $n = 1$ and 2 the results are equivalent to those

for an infinite lattice with coordination number $z = 4$ and 5 respectively. Hence we will assume here that n is larger than 3.

For the antiferromagnetic Ising phase the situation is as follows. The staggered magnetization, $\bar{m}_r$ for each layer, gives rise to w different 'order' parameters. The quantities δ_r^{xx} and δ_r^{zz} give an additional $w-1$ parameters. There is no $\delta_w^{\alpha\alpha}$, since for even n the layers w and $w+1$ are equivalent because of the reflection symmetry, and hence $\delta_w^{\alpha\alpha} = 0$, and for odd n, $\delta_w^{\alpha\alpha} = \delta_{w-1}^{\alpha\alpha}$. So in total the vector c contains $3w-2$ parameters connected with the antiferromagnetic Ising phase; these elements of c will be ordered as follows:

$$\begin{aligned} c_{3r-2} &= \bar{m}_r \qquad (r = 1, \ldots, w) \\ c_{3r-1} &= \delta_r^{xx} \qquad (r = 1, \ldots, w-1) \\ c_{3r} &= \delta_r^{zz} \qquad (r = 1, \ldots, w-1)\,. \end{aligned} \tag{A1}$$

In this notation the elements of $\mathbf{M}^{\mathrm{AI}}$ are, for $r < w$:

$$M_{1,1}^{\mathrm{AI}} = \frac{-8}{1-m_1^2} + \frac{2}{c_{1\parallel}^{xx}} \ln \frac{\lambda_{1\parallel 2}^0}{\lambda_{1\parallel 3}^0} + \tfrac{1}{2}\left(\alpha_1^+ + \frac{\Delta_1^2}{\omega_1^2}\beta_1^+\right) + \frac{1}{4\omega_1}\left(1 - \frac{\Delta_1^2}{\omega_1^2}\right)\gamma_1$$

$$M_{3r-2,3r-2}^{\mathrm{AI}} = \frac{-10}{1-m_r^2} + \frac{2}{c_{r\parallel}^{xx}} \ln \frac{\lambda_{r\parallel 2}^0}{\lambda_{r\parallel 3}^0} + \tfrac{1}{2}\left(\alpha_r^+ + \frac{\Delta_r^2}{\omega_r^2}\beta_r^+\right) + \frac{1}{4\omega_r}\left(1 - \frac{\Delta_r^2}{\omega_r^2}\right)\gamma_r$$
$$+ \tfrac{1}{2}\left(\alpha_{r-1}^+ + \frac{\Delta_{r-1}^2}{\omega_{r-1}^2}\beta_{r-1}^+\right) + \frac{1}{4\omega_{r-1}}\left(1 - \frac{\Delta_{r-1}^2}{\omega_{r-1}^2}\right)\gamma_{r-1} \qquad (r \neq 1)$$

$$M_{3r-2,3r-1}^{\mathrm{AI}} = \frac{\Delta_r c_{r\perp}^{xx}}{\omega_r^2}\beta_r^+ - \frac{\Delta_r c_{r\perp}^{xx}}{2\omega_r^3}\gamma_r$$

$$M_{3r-2,3r}^{\mathrm{AI}} = \tfrac{1}{2}\left(\alpha_r^- - \frac{\Delta_r}{\omega_r}\beta_r^-\right)$$

$$M_{3r-2,3r+1}^{\mathrm{AI}} = -\tfrac{1}{2}\left(\alpha_r^+ - \frac{\Delta_r^2}{\omega_r^2}\beta_r^+\right) + \frac{1}{4\omega_r}\left(1 - \frac{\Delta_r^2}{\omega_r^2}\right)\gamma_r \tag{A2}$$

$$M_{3r-1,3r-1}^{\mathrm{AI}} = \frac{c_{r\perp}^{xx\,2}}{\omega_r^2}\beta_r^+ + \frac{1}{\omega_r}\left(1 - \frac{c_{r\perp}^{xx\,2}}{\omega_r^2}\right)\gamma_r$$

$$M_{3r-1,3r}^{\mathrm{AI}} = -\frac{c_{r\perp}^{xx}}{\omega_r}\beta_r^-$$

$$M_{3r-1,3r+1}^{\mathrm{AI}} = M_{3r-2,3r-1}^{\mathrm{AI}}$$

$$M_{3r,3r}^{\mathrm{AI}} = \tfrac{1}{2}(\alpha_r^+ + \beta_r^+)$$

$$M_{3r,3r+1}^{\mathrm{AI}} = -\tfrac{1}{2}\left(\alpha_r^- + \frac{\Delta_r}{\omega_r}\beta_r^-\right).$$

From the last layer there is, for even n, a contribution

$$M_{3w-2,3w-2}^{\mathrm{AI}} = \frac{-10}{1-m_w^2} + \frac{2}{c_{w\parallel}^{xx}} \ln \frac{\lambda_{w\parallel 2}^0}{\lambda_{w\parallel 3}^0} + \frac{1}{2c_{w\perp}^{xx}} \ln \frac{\lambda_{w\perp 2}^0}{\lambda_{w\perp 3}^0}$$
$$+ \tfrac{1}{2}\left(\alpha_{w-1}^+ + \frac{\Delta_{w-1}^2}{\omega_{w-1}^2}\beta_{w-1}^+\right) + \frac{1}{4\omega_{w-1}}\left(1 - \frac{\Delta_{w-1}^2}{\omega_{w-1}^2}\right)\gamma_{w-1} \tag{A3a}$$

and for odd n

$$M^{\mathrm{AI}}_{3w-2,3w-2} = \frac{-5}{1-m_w^2} + \frac{1}{c^{xx}_{w\|}} \ln \frac{\lambda^0_{w\| 2}}{\lambda^0_{w\| 3}} + \tfrac{1}{2}\left(\alpha^+_{w-1} + \frac{\Delta^2_{w-1}}{\omega^2_{w-1}}\beta^+_{w-1}\right) + \frac{1}{4\omega_{w-1}}\left(1 - \frac{\Delta^2_{w-1}}{\omega^2_{w-1}}\right)\gamma_{w-1}. \qquad \text{(A3}b\text{)}$$

The following definitions have been used

$$\begin{aligned} \alpha^{\pm}_r &= \frac{1}{4\lambda^0_{r\perp 1}} \pm \frac{1}{4\lambda^0_{r\perp 4}} \\ \beta^{\pm}_r &= \frac{1}{4\lambda^0_{r\perp 2}} \pm \frac{1}{4\lambda^0_{r\perp 3}} \\ \gamma_r &= \ln \frac{\lambda^0_{r\perp 2}}{\lambda^0_{r\perp 3}} \\ \Delta_r &= \tfrac{1}{2}(m_r - m_{r+1}) \\ \omega_r &= \sqrt{\Delta_r^2 + c^{xx\,2}_{r\perp}}. \end{aligned} \qquad \text{(A4)}$$

In the x–y ordered phase there are w parameters c^x_r and $c^{xz}_{r\|}$ and $w-1$ different parameters $c^{xz}_{r\perp}$ and $c^{zx}_{r\perp}$. Finally, if n is even, there is one additional parameter $c^{xz}_{w\perp} = c^{zx}_{w\perp}$ because of the reflection symmetry. So in total c contains $4w-2$ parameters for odd n, $4w-1$ for even n, ordered as follows:

$$\begin{aligned} c_{4r-3} &= c^x_r && (r = 1, \ldots, w) \\ c_{4r-2} &= c^{xz}_{r\|} && (r = 1, \ldots, w) \\ c_{4r-1} &= c^{xz}_{r\perp} && (r = 1, \ldots, w-1) \\ c_{4r} &= c^{zx}_{r\perp} && (r = 1, \ldots, w-1) \\ c_{4w-1} &= c^{xz}_{w\perp} && (\text{for } n \text{ even}). \end{aligned} \qquad \text{(A5)}$$

For the matrix M^{XY} we find, for $r < w$

$$M^{\mathrm{XY}}_{1,1} = -\frac{8}{m_1}\ln\frac{1+m_1}{1-m_1} + 8\left(\ell^{1\|}_{12} + \ell^{1\|}_{24}\right) + \frac{2}{1+\xi_1^2}\left[\xi_1^2\left(\ell^{1\perp}_{12} + \ell^{1\perp}_{34}\right) + \ell^{1\perp}_{13} + \ell^{1\perp}_{24}\right]$$

$$M^{\mathrm{XY}}_{4r-3,4r-3} = -\frac{10}{m_r}\ln\frac{1+m_r}{1-m_r} + 8\left(\ell^{r\|}_{12} + \ell^{r\|}_{24}\right) + \frac{2}{1+\xi_r^2}\left[\xi_r^2\left(\ell^{r\perp}_{12} + \ell^{r\perp}_{34}\right) + \ell^{r\perp}_{13} + \ell^{r\perp}_{24}\right] + \frac{2}{1+\xi_{r-1}^2}\left[\xi_{r-1}^2\left(\ell^{r-1\perp}_{13} + \ell^{r-1\perp}_{24}\right) + \ell^{r-1\perp}_{12} + \ell^{r-1\perp}_{34}\right] \qquad (r \neq 1) \qquad \text{(A6}a\text{)}$$

$$M^{XY}_{4r-3,4r-2} = 8\left(\ell^{r\parallel}_{12} - \ell^{r\parallel}_{24}\right)$$

$$M^{XY}_{4r-3,4r-1} = \frac{2}{1+\xi_r^2}\left[\xi_r^2\left(\ell^{r\perp}_{12} - \ell^{r\perp}_{34}\right) + \ell^{r\perp}_{13} - \ell^{r\perp}_{24}\right]$$

$$M^{XY}_{4r-3,4r} = \frac{2\xi_r}{1+\xi_r^2}\left(\ell^{r\perp}_{12} + \ell^{r\perp}_{34} - \ell^{r\perp}_{13} - \ell^{r\perp}_{24}\right)$$

$$M^{XY}_{4r-3,4r+1} = \frac{2\xi_r}{1+\xi_r^2}\left(\ell^{r\perp}_{12} - \ell^{r\perp}_{34} - \ell^{r\perp}_{13} + \ell^{r\perp}_{24}\right)$$

$$M^{XY}_{4r-2,4r-2} = 8\left(\ell^{r\parallel}_{12} + \ell^{r\parallel}_{24}\right)$$

$$M^{XY}_{4r-1,4r-1} = \frac{2}{1+\xi_r^2}\left[\xi_r^2\left(\ell^{r\perp}_{12} + \ell^{r\perp}_{34}\right) + \ell^{r\perp}_{13} + \ell^{r\perp}_{24}\right] \tag{A6b}$$

$$M^{XY}_{4r-1,4r} = \frac{2\xi_r}{1+\xi_r^2}\left[\ell^{r\perp}_{12} - \ell^{r\perp}_{34} - \ell^{r\perp}_{13} + \ell^{r\perp}_{24}\right]$$

$$M^{XY}_{4r-1,4r+1} = \frac{2\xi_r}{1+\xi_r^2}\left[\ell^{r\perp}_{12} + \ell^{r\perp}_{34} - \ell^{r\perp}_{13} - \ell^{r\perp}_{24}\right]$$

$$M^{XY}_{4r,4r} = \frac{2}{1+\xi_r^2}\left[\xi_r^2\left(\ell^{r\perp}_{13} + \ell^{r\perp}_{24}\right) + \ell^{r\perp}_{12} + \ell^{r\perp}_{34}\right]$$

$$M^{XY}_{4r,4r+1} = \frac{2}{1+\xi_r^2}\left[\xi_r^2\left(\ell^{r\perp}_{13} - \ell^{r\perp}_{24}\right) + \ell^{r\perp}_{12} - \ell^{r\perp}_{34}\right] .$$

The last few elements are, for even n

$$M^{XY}_{4w-3,4w-3} = -\frac{10}{m_w}\ln\frac{1+m_w}{1-m_w} + 8\left(\ell^{w\parallel}_{12} + \ell^{w\parallel}_{24}\right) + 2\left(\ell^{w\perp}_{12} + \ell^{w\perp}_{24}\right)$$
$$+ \frac{2}{1+\xi_{w-1}^2}\left[\xi_{w-1}^2\left(\ell^{w-1\perp}_{13} + \ell^{w-1\perp}_{24}\right) + \ell^{w-1\perp}_{12} + \ell^{w-1\perp}_{34}\right]$$

$$M^{XY}_{4w-3,4w-2} = 8\left(\ell^{w\parallel}_{12} - \ell^{w\parallel}_{24}\right)$$

$$M^{XY}_{4w-3,4w-1} = 2\left(\ell^{w\perp}_{12} - \ell^{w\perp}_{24}\right) \tag{A7a}$$

$$M^{XY}_{4w-2,4w-2} = 8\left(\ell^{w\parallel}_{12} + \ell^{w\parallel}_{24}\right)$$

$$M^{XY}_{4w-1,4w-1} = 2\left(\ell^{w\perp}_{12} + \ell^{w\perp}_{24}\right)$$

and for odd n

$$M^{XY}_{4w-3,4w-3} = -\frac{5}{m_w}\ln\frac{1+m_w}{1-m_w} + 4\left(\ell^{w\parallel}_{12} + \ell^{w\parallel}_{24}\right)$$
$$+ \frac{2}{1+\xi_{w-1}^2}\left[\xi_{w-1}^2\left(\ell^{w-1\perp}_{13} + \ell^{w-1\perp}_{24}\right) + \ell^{w-1\perp}_{12} + \ell^{w-1\perp}_{34}\right]$$

$$M^{XY}_{4w-3,4w-2} = 4\left(\ell^{w\parallel}_{12} - \ell^{w\parallel}_{24}\right) \tag{A7b}$$

$$M^{XY}_{4w-2,4w-2} = 4\left(\ell^{w\parallel}_{12} + \ell^{w\parallel}_{24}\right) .$$

We have used the definitions

$$\xi_r = \left(\frac{(c_r^z - c_{r+1}^z)^2}{4c_{r\perp}^{xx\,2}} + 1\right)^{1/2} - \frac{(c_r^z - c_{r+1}^z)}{2c_{r\perp}^{xx}}$$
$$\ell_{km}^{r\zeta} = \frac{\ln(\lambda_{r\zeta\,k}^0/\lambda_{r\zeta\,m}^0)}{4(\lambda_{r\zeta\,k}^0 - \lambda_{r\zeta\,m}^0)} \qquad (\zeta = \|, \perp)\,. \tag{A8}$$

Finally, if $h = 0$, there are w parameters m_r for the ferromagnetic Ising phase, giving a vector c:

$$c_r = m_r \qquad (r = 1, \ldots, w) \tag{A9}$$

and a matrix M^{FI} (for $r < w$):

$$M_{1,1}^{\mathrm{FI}} = -8 + \frac{8}{1 + c_{1\|}^{zz}} + \frac{1}{1 + c_{1\perp}^{zz}} + \frac{1}{4c_{1\perp}^{xx}} \ln \frac{\lambda_{1\perp 2}^0}{\lambda_{1\perp 3}^0}$$
$$M_{r,r}^{\mathrm{FI}} = -10 + \frac{8}{1 + c_{r\|}^{zz}} + \frac{1}{1 + c_{r\perp}^{zz}} + \frac{1}{4c_{r\perp}^{xx}} \ln \frac{\lambda_{r\perp 2}^0}{\lambda_{r\perp 3}^0} + \frac{1}{1 + c_{r-1\perp}^{zz}}$$
$$+ \frac{1}{4c_{r-1\perp}^{xx}} \ln \frac{\lambda_{r-1\perp 2}^0}{\lambda_{r-1\perp 3}^0} \qquad (r \neq 1) \tag{A10}$$
$$M_{r,r+1}^{\mathrm{FI}} = \frac{1}{1 + c_{r\perp}^{zz}} - \frac{1}{4c_{r\perp}^{xx}} \ln \frac{\lambda_{r\perp 2}^0}{\lambda_{r\perp 3}^0}$$

while for $r = w$ and n even we find

$$M_{w,w}^{\mathrm{FI}} = -10 + \frac{8}{1 + c_{w\|}^{zz}} + \frac{2}{1 + c_{w\perp}^{zz}} + \frac{1}{1 + c_{w-1\perp}^{zz}} + \frac{1}{4c_{w-1\perp}^{xx}} \ln \frac{\lambda_{w-1\perp 2}^0}{\lambda_{w-1\perp 3}^0} \tag{A11a}$$

and for n odd

$$M_{w,w}^{\mathrm{FI}} = -5 + \frac{4}{1 + c_{w\|}^{zz}} + \frac{1}{1 + c_{w-1\perp}^{zz}} + \frac{1}{4c_{w-1\perp}^{xx}} \ln \frac{\lambda_{w-1\perp 2}^0}{\lambda_{w-1\perp 3}^0}\,. \tag{A11b}$$

References

[1] Fisher M E 1967 *Rep. Prog. Phys.* **30** 615
[2] Matsubara T and Matsuda H 1956 *Prog. Theor. Phys.* **16** 569
Matsuda H and Matsubara T 1957 *Prog. Theor. Phys.* **17** 19
[3] Matsuda H and Tsuneto T 1970 *Prog. Theor. Phys. Suppl.* **46** 411
[4] Liu K-S and Fisher M E 1973 *J. Low Temp. Phys.* **10** 655
[5] Robaszkiewicz S, Micnas R, and Chao K A 1981 *Phys. Rev.* B **23** 1447
[6] Micnas R, Ranninger J, and Robaszkiewicz S 1990 *Rev. Mod. Phys.* **62** 113
[7] de Jongh L J 1989 *Physica* C **161** 631
[8] Manousakis E 1991 *Rev. Mod. Phys.* **63** 1
[9] Kikuchi R 1951 *Phys. Rev.* **81** 988
[10] Morita T 1972 *J. Math. Phys.* **13** 115

[11] An G 1988 *J. Stat. Phys.* **52** 727
[12] Katsura S and Shimada K 1980 *Phys. Status Solidi* b **102** 163
[13] Bukman D J, An G, and van Leeuwen J M J 1991 *Phys. Rev.* B **43** 13352
[14] Schick M and Siddon R L 1973 *Phys. Rev.* A **8** 339
[15] Maritan A, Langie G, and Indekeu J O 1991 *Physica* A **170** 326
[16] Huhn W and Dohm V 1988 *Phys. Rev. Lett.* **61** 1368
Schmolke R, Wacker A, Dohm V, Franck D 1990 *Physica* B **165–166** 575
[17] Capehart T W and Fisher M E 1976 *Phys. Rev.* B **13** 5021
[18] Mermin N D and Wagner H 1966 *Phys. Rev. Lett.* **17** 1133
[19] Jasnow D and Fisher M E 1971 *Phys. Rev.* B **3** 895
Fisher M E and Jasnow D 1971 *Phys. Rev.* B **3** 907
[20] Kosterlitz J M and Thouless D J 1973 *J. Phys. C: Solid State Phys.* **6** 1181
[21] Parga N and van Himbergen J E 1981 *Ann. Phys.* **134** 286
[22] Rushbrooke G S, Baker G A Jr and Wood P J 1974 *Phase Transitions and Critical Phenomena* vol 3, ed C Domb and M S Green (New York: Academic)
Betts D D 1974 *Phase Transitions and Critical Phenomena* vol 3, ed C Domb and M S Green (New York: Academic)
Domb C 1974 *Phase Transitions and Critical Phenomena* vol 3, ed C Domb and M S Green (New York: Academic)
Rogiers J, Grundke E W and Betts D D 1979 *Can. J. Phys.* **57** 1719